

Shell evolution towards ^{60}Ca : First spectroscopy of $^{62}\text{Ti}^\dagger$

M. L. Cortés,^{*1,*2} W. Rodríguez,^{*1,*3} P. Doornenbal,^{*1} A. Obertelli,^{*4,*5} J. D. Holt,^{*6} S. M. Lenzi,^{*7} J. Menéndez,^{*8} F. Nowacki,^{*9} K. Ogata,^{*10,*11} A. Poves,^{*12} T. R. Rodríguez,^{*12} A. Schwenk,^{*5,*13,*14} J. Simonis,^{*15} S. R. Stroberg,^{*6,*16} and K. Yoshida^{*17} for the SEASTAR2017 collaboration.

The study of $N = 40$ isotones can provide insight into the mechanisms governing shell evolution. Along this isotonic chain different behaviors are observed: ^{68}Ni shows a high $E(2_1^+)$ and a low $B(E2)_{\downarrow}$.¹⁾ For Fe and Cr, a monotonous decrease of the $E(2_1^+)$ when approaching $N = 40$ has been observed,¹⁾ while the $E(2_1^+)$ of $^{58,60}\text{Ti}$ shows a moderate decrease towards $N = 40$.^{2,3)} The very exotic ^{60}Ca , where the Ca isotopic chain meets the $N = 40$ isotones, is difficult to reach experimentally and only recently its existence has been established.⁴⁾ Theoretical calculations in the shell-model framework⁵⁾ concluded that quadrupole correlations in the $N = 40$ isotopes give rise to deformed ground states dominated by intruder neutron orbits beyond the pf shell, leading to an island of inversion below ^{68}Ni . On the other hand, symmetry conserving configuration mixing calculations with the Gogny interaction predict a conservation of the $N = 40$ gap leading to spherical ^{62}Ti and ^{60}Ca .⁶⁾ In this work, the first spectroscopy of ^{62}Ti is presented.

A 345 MeV/nucleon beam of ^{70}Zn with an average intensity of 240 pnA was fragmented on a Be target to produce ^{63}V . The isotopes were identified using BigRIPS⁷⁾ and delivered to the 151.3(13) mm long liquid hydrogen target of MINOS⁸⁾ placed in front of the SAMURAI magnet. Outgoing ^{62}Ti fragments were identified using SAMURAI and associated detectors.⁹⁾ MINOS was surrounded by DALI2⁺, composed of 226 NaI(Tl) detectors.^{10,11)}

Two peaks were clearly identified in the Doppler corrected γ -spectrum, and were found to be in coincidence. Using a 2-dimensional χ^2 minimization the energies of the transitions were deduced to be 683(10) keV and 823(20) keV, which were tentatively assigned to the $2_1^+ \rightarrow 0_{\text{gs}}^+$ and $4_1^+ \rightarrow 2_1^+$ transitions, respectively. The evolution of measured $E(2_1^+)$ and $E(4_1^+)$ energies for the

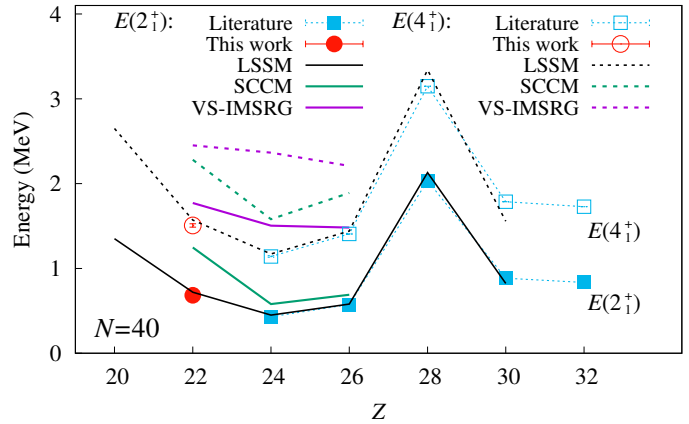


Fig. 1. Systematics of $E(2_1^+)$ and $E(4_1^+)$ for even-even $N = 40$ isotones, including the present measurement. The black, green, and purple lines represent LSSM, SCCM, and VS-IMSRG calculations, respectively.

$N = 40$ isotones between Ti and Ge¹⁾ is presented in Fig. 1. The $E(2_1^+)$ and $E(4_1^+)$ of ^{62}Ti have a similar value than the ones measured for ^{66}Fe , higher than those of ^{64}Cr . This shows the first increase of $E(2_1^+)$ along the $N = 40$ isotones towards ^{60}Ca . Large Scale Shell Model (LSSM) calculations using the LNPS interaction reproduce very accurately the data, indicating that the island of inversion in this region extends down to ^{60}Ca . Symmetry conserving configuration mixing (SCCM) calculations using the Gogny D1S effective interaction predict $E(2_1^+)$ for ^{64}Cr and ^{66}Fe which lie very close to the LSSM predictions. However, for ^{62}Ti a larger increase of the $E(2_1^+)$ is obtained. For the $E(4_1^+)$ energies, the calculations overestimate the experimental values by about 500 keV, although the minimum value for ^{64}Cr is maintained. Ab initio valence-space in-medium similarity renormalization group (VS-IMSRG) calculations overestimate the $E(2_1^+)$ and $E(4_1^+)$ excitation energies in ^{62}Ti , ^{64}Cr , and ^{66}Fe , predicting all states as spherical.

References

- 1) <http://www.nndc.bnl.gov/ensdf/>.
- 2) H. Suzuki *et al.*, Phys. Rev. C **88**, 024326 (2013).
- 3) A. Gade *et al.*, Phys. Rev. Lett. **112**, 112503 (2014).
- 4) O. B. Tarasov *et al.*, Phys. Rev. Lett. **121**, 022501 (2018).
- 5) S. M. Lenzi *et al.*, Phys. Rev. C **82**, 054301 (2010).
- 6) T. R. Rodríguez *et al.*, Phys. Rev. C **93**, 054316 (2016).
- 7) T. Kubo *et al.*, Prog. Theor. Exp. Phys. **2012**, (2012).
- 8) A. Obertelli *et al.*, Eur. Phys. J. A **50**, (2014).
- 9) T. Kobayashi *et al.*, Nucl. Instrum. Methods Phys. Res. B **317**, 294 (2013).
- 10) S. Takeuchi *et al.*, Nucl. Instrum. Methods Phys. Res. A **763**, 596 (2014).
- 11) I. Murray *et al.*, RIKEN Accel. Prog. Rep. **51**, 158 (2017).

[†] Condensed from Phys. Lett. B **800**, 135071 (2020)

^{*1} RIKEN Nishina Center

^{*2} INFN-Laboratori Nazionali di Legnaro

^{*3} Universidad Nacional de Colombia

^{*4} IRFU, CEA, Université Paris-Saclay

^{*5} Institut für Kernphysik, Technische Universität Darmstadt
^{*6} TRIUMF

^{*7} Dipartimento di Fisica e Astronomia, Università di Padova

^{*8} Center for Nuclear Study, The University of Tokyo

^{*9} IPHC, CNRS/IN2P3, Université de Strasbourg

^{*10} RCNP, Osaka University

^{*11} Department of Physics, Osaka City University

^{*12} Departamento de Física Teórica, Universidad Autónoma de Madrid

^{*13} EMMI, GSI Helmholtzzentrum für Schwerionenforschung

^{*14} Max-Planck-Institut für Kernphysik

^{*15} Institut für Kernphysik, Johannes Gutenberg-Universität

^{*16} Department of Physics, University of Washington

^{*17} Advanced Science Research Center, Japan Atomic Energy Agency